MeerKAT L Band Polarimetric Calibration

A. Plavin (NRAO), W. D. Cotton (NRAO), T. Mauch (SARAO) January 17, 2020

***Abstract*—After application of cross polarized phase calibration using the noise diodes, the MeerKAT L band polarization charactersics appear quite stable. A standard calibration procedure appears to be able to at least approximately calibrate existing L band archive data. Calibration of commissioning and science verification data from the archive is discussed and examples are given. Suggestions for polarization calibration of MeerKAT data are given. Two additional L Band polarized calibrators are suggested, J1130-1449 and J2329-4730.**

***Index Terms*—MeerKAT polarimetry**

I. Introduction

POLARIMETRY using the MeerKAT array has the potential to produce valuable scientific results both for the understanding of polarized emission from AGNs and other synchrotrn emittiong sources as well as probing the magnetoionic medium on the path between us and the source. The standard correlation products from MeerKAT include all four products of the two orthogonal linearly polarized feeds on each antenna allows the recovery of the full polarization state of the incoming radiation. These data suffer from a number of propagation and instrumental corruptions which need to be corrected. This memo discusses a procedure for correcting instrumental corruptions using the Obit package [1] [1].

II. Polarimetry Using Linear Feeds

A. Leakage

To first order, the interferometric response for an interferometer between antennas j and k using linear detectors of an unresolved source is [2]:

$$v_{XX} = \frac{1}{2} g_{jX} g^*_{kX} (I + Q\cos2\chi + U\sin2\chi),$$

$$v_{XY} = \frac{1}{2} g_{jX} g^*_{kY} [(d_{jX} + d^*_{kY})I - Q\sin2\chi + U\cos2\chi + iV)], \quad (1)$$

$$v_{YX} = \frac{1}{2} g_{jY} g^*_{kX} [(d_{jY} + d^*_{kX})I - Q\sin2\chi + U\cos2\chi - iV)],$$

$$v_{YY} = \frac{1}{2} g_{jY} g^*_{kY} (I - Q\cos2\chi - U\sin2\chi),$$

where g_{jp} is the complex gain of the electronics for polarization p on antenna j, "*" denotes the complex conjugate, I, Q, U, and V are the Stokes parameters of the source emission, the d_X and d_Y terms are the "leakage" of Y into X and X into Y, i is $\sqrt{-1}$ and, χ is the parallactic angle given by:

$$\chi = \tan^{-1}\Big(\frac{\cos\lambda \sin h}{\sin\lambda\cos\delta - \cos\lambda\sin\delta\cos h}\Big) \quad (2)$$

where δ is the source declination, λ is the latitude of the antenna and h is the hour angle of the source. Calibration consists of determining the g and d terms.

An equivalent formulation can be developed in terms of the ellipticity and orientation of the emission radiated from each feed, [2], [3]. This formulation doesn't have a first order version but has the advantage that for linear feeds, one of the parameters can be measured, in principle, using a plumb bob and a protractor.

B. Leakage vs. source polarization

Equation (1) shows that leakage (d) adds a fraction of Stokes I to the cross hand polarizations. In the case that parallel–hand calibration and cross hand phase calibration has been applied (g=1+0i), and the d terms are zero, the expectations of the real part of the cross–hand correlations are the same value and the ratio of the real parts can be used as a diagnostic. The two "orthogonal" polarizations of an antenna are, in general, quite close to orthogonal although not necessarily the desired polarization state. This means that the defects from perfect polarization, the d terms, are close to the negative of each other for the two hands of a feed. Consider the case where one antenna of a baseline has a perfect feed (d=0) and the other signigicant leakage, (real(d_X)=leak=-real(d_Y)). In this case, the real parts of the cross–hand correlations become

$$-Q\sin2\chi + U\cos2\chi \ \pm \ leak \times I$$

which effectively doubles the effect of the leakage. If d terms of the two antennas are the negatives of each other, then the real part of the cross hand polarizations become

$$-Q\sin2\chi + U\cos2\chi \ \pm \ 2leak \times I$$

thus effectively quadrupling the effect of leakage. A leakage of 2.5% can in the right circumstances have the same effect on the cross–hand real ratio as a 10% source polarization degrading the usefulness of the cross–hand real ratio as a disgnostic.

III. SVD Analysis

Assuming no direction-dependent effects, the uncalibrated complex visibilities on baseline between antennas i and j are

$$V_{ijp'q'} = \sum_{p,q} J_{ip'p} S_{ijpq} J^*_{jq'q} + \varepsilon_{ijp'q'},$$

where S — true source visibilities, J_i — 2x2 Jones matrix for antenna i, * represents complex conjugate, p, q — two basis directions in the polarization space (e.g. two orthogonal linear polarization, X and Y), p', q' — antenna feed indices (for MeerKAT, with close-to-linear feeds, we call them X and Y). This equation is often called RIME - Radio Interferemoter Measurement Equation.

National Radio Astronomy Observatory, 520 Edgemont Rd., Charlottesville, VA, 22903 USA email: bcotton@nrao.edu

South African Radio Astronomy Observatory, 2 Fir St., Observatory, South Africa

[1] http://www.cv.nrao.edu/∼bcotton/Obit.html

If the source (calibrator) is a point-source in the phase center, then its true visibilities do not depend on the baseline, i.e. $S_{ijpq} = S_{pq}$, a 2x2 matrix. Then the measurement equation is a simple matrix multiplication:

$$V = JSJ^*,$$

where V is a $2n_{\rm ant} \times 2n_{\rm ant}$ matrix with indices ip', jq', J — a $2n_{\rm ant} \times 2$ matrix with indices ip', p, and * is conjugate transpose.

A well-known fact is that a single observation of a single source with unknown properties S is not enough to usefully constrain the J and S matrices in this equation. So we propose the following general procedure, which gives simple ways to introduce various a-priori known information about the calibrator, and about the antennas themselves.

- Represent visibility matrix of each scan (indexed with k) independently as $V_k = U_k U_k^*$ using truncated SVD (Singular Value Decomposition). Here each U_k is a $2n_{\rm ant} \times 2$ matrix with indices ip', p. Generally, $U_k = Js_k$, where $s_k s_k^*$ — true visibilities in the scan k. Further we use the notation $s = S^{1/2}$ meaning that $S = ss^*$.
  Note, that if the source is completely unpolarized, $s_k \sim I$. In this case the U matrices already give a solution for the instrumental properties, up to inherent ambiguties. However, we continue with our general formulation.
  Already in this step we use the assumption that the source is point-like. Fairness of this assumption can be evaluated by directly examining residuals $V_k - U_k U_k^*$, or looking at singular values 1 and 2 compared to all remaining ones (from 3 to $2n_{\rm ant}$).
- Gather U_k matrices from all scans and all calibrators into one $2n_{\rm ant} \times 2n_{\rm scan}$ matrix U. As each $U_k = Js_k$, the combined matrix is $U = Js$, where s is a $2 \times 2n_{\rm scan}$ matrix containing the concatenation of s_k matrices.
  Applying truncated SVD to this U matrix gives us the following decomposition: $U = J's'$. The apostrophes indicate the inherent ambiguity still remaining: we can take any invertible matrix X and replace J with JX^{-1}, s with Xs without changing the observed visibilities.
  Resolving these ambiguities requires additional information, as the visibilities themselves do not allow us to choose the correct solution. There are many possible ways to proceed here, and we propose a particular interpretable pipeline, which starts from the computed J' and s' matrices.
- Take s'_k matrices for all scans of an unpolarized calibrator and compute corresponding $S'_k = s'_k s'^*_k$ — uncalibrated source visibilities. They should be almost the same, up to noise and instrumental variations, so we average them all into a single 2×2 $S'_{\rm unpolar}$ matrix. As the source is unpolarized, we know that the calibrated visibilities is a scaled identity matrix — $S_{\rm unpolar} \propto I$. So, taking $X = {s'_{\rm unpolar}}^{-1/2}$ transforms the source matrix to the correct one.
  This step reduces the ambiguity, but does not eliminate it: we can still take the X transformation matrix to be any $2x2$ unitary one. This is and expected and well-known ambiguity when using an unpolarized calibrator alone. However, after this step the total polarization fraction (sum of linear and circular) is correct — see Hamaker for details.
- There are several approaches possible for calibrating the linear polarization direction (EVPA). Some options include measuring the feed directions in some way, i.e. mechanically at the antenna site, or using a source with a known EVPA direction. Here we assume that on average, antenna feeds have the same direction as designed: X-feeds are aligned with the meridian, and Y-feeds are orthogonal to it.
  We implement this constrain mathematically with the X transformation matrix calculated analytically from $J'_{\rm avg}$ — a 2×2 average of intermediate "Jones matrices" J'. Denote individual elements of $J'_{\rm avg}$ as w, x, y, z: $J'_{\rm avg} = \begin{bmatrix} w & x \\ y & z \end{bmatrix}$. In order to get rid of rotation here, the transform should consist of a rotation matrix and a phase shift: $X = \begin{bmatrix} c & s \\ -s & c \end{bmatrix} Diag[1, p]$. The values are computed as follows: $c = \sqrt{\frac{1}{1+t^2}}, s = t \cdot c$, $t = mean(\|\frac{x}{w}\|, \|\frac{y}{z}\|)$, $p = norm(mean(\frac{x}{w}, \left(\frac{-y}{z}\right)^*))$.
- Another remaining ambiguity is the linear versus circular polarization confusion. This amount to a phase shift between X and Y signals, or a diagonal Jones matrix $diag[1, p]$. A way to calibrate for this effect consists of observing a linearly-polarized source without circular polarization. Source visibility matrix S in this case should have pure real offdiagonal terms. This constrain can easily be implemented by taking the phase correction multiplier above $p = norm(RMS_k({S'_{k,12}}^2))$ or similarly with the other offdiagonal element S'_{21} instead of S'_{12}.
- There is only one phase-related ambigity remaining after the previous steps, and that is the sign, or $180°$ phase shift in cross-hand XY and YX visibilities. This can reliably be resolved using a linearly-polarized source with even a very roughly known EVPA direction. One needs to test two possibilities: the transormation matrix $X = diag[1, 1]$ or $X = diag[1, -1]$, and choose the one giving closer EVPA to the a-priori known one.
- It remains to put the measurements onto the correct absolute amplitude scale. This can be done e.g. using a source with known flux density, or assuming that amplitude scale was calibrated correctly a-priori. We take the latter approach here, which amounts to getting moduli of diagonal values in Jones matrices as close to unity as possible. Mathematically, we just take $X = \langle J'_{i,pp} \rangle_{i,p}$.

IV. Calibration pipeline

The KATObitPipe Obit based MeerKAT continuum calibration pipeline which is used to obtain data from the archive, edit corrupted data and determine and apply parallel–hand calibration also has an option (-polcal) for calibrating data for which polarmetry is desired. These options are designed primarily to determine and maintain the frequency dependent phase difference between the X and Y (AKA H and V) feed systems

to which the parallel–hand calibration is relatively insensitive. The basic calibration steps are given in the following; there are also numerous editing steps looking for outliers in either the data or calibration solutions which are not explicltly described here.

1) **Download from archive:** Data are download from the archive into an AIPS format dataset with optional application of various editing options. Data are arbitrarily divided into 8 AIPS "IFs" to aid in the calibration.
2) **Hann:** The data are Hanning smoothed to reduce the effects of the inpulsive RFI and to reduce the number of spectral channels by a factor of two.
3) **X–Y phase calibration:** Cross polarized autocorrelations of data with the noise diodes injected into the signal path made at the beginning of an observing session are used in program MKXPhase to determine the phase difference in each channel for each antenna. These are written in the form of an AIPS BP table and applied to the data prior to each subseqent calibration step.
4) **Pick reference antenna:** A test calibration is done on a bandpass calibrator and the antenna with the most significant solutions is chosen as the reference antenna in subsequent calibration steps needing one. A specific antenna can also be specified.
5) **Delay Calibration:** The strong, bandpass calibration sources are used to determine group delay and phase offsets in each "IF". A sky and frequency model of the calibrator is used in this calibration and the solutions are averaged in polarization to maintain the X-Y phase relationship. The solutions are averaged in XX and YY.
6) **Bandpass Calibration:** The bandpass calibrations are used to determine gains in each channel, polarization and antenna using sky and spectral models of the calibrator. This is best done using 1934-638 which is very weakly polarized. The AIPS BP table from this proess is multiplied by the one from MKXPhase and used is subsequent steps.
7) **Amplitude and phase calibration:** Gain solutions averaging the XX and YY data are obtained for the flux density calibrators and phase reference sources, using source models and standard spectra when available. The flux densities of the phase reference sources are determined by a comparison with the solutions of the flux density calibrators and the corrected solutions applied to all data.
8) **Rinse and repeat:** The derived calibration tables are deleted but the editing table (AIPS FG) derived in the preceeding is kept and the calibration repeated. This assures that the calibration is based on well edited data.
9) **Apply calibration and average:** The derived calibration and editing tables are applied and the data time averaged in a baseline dependent fashion to avoid distorting the desired field of view and averaged in frequency. The resultant data are written to a FITS file.

V. Polarimetry in Obit

Obit stores calibration parameters in separate tables from the data and then applies them as needed. The tables and software relevant for polarimetry are the following:

- **AIPS PD:** The AIPS PD table contains channel/IF and antenna specific polarization characterization parameters. Feed ellipticity and orientation is the preferred parameterization. Application of an AIPS PD table also transforms the visibility data to a circular basis. Task PCal writes these tables.
- **AIPS BP:** The AIPS BP table contains channel/IF, polarization and antenna specific complex gains. X-Y phase offsets are stored as the phase of the Y polarization. Amplitude ratios can also be saved. Task PCal uses these tables for fitted residual X–Y phase differences and X/Y gain ratios. Task RLPass can generate an AIPS BP table to correct the R-L phase difference for data in a circular basis.
- **AIPS SN/CL:** X–Y phase and delay offsets can be saved in AIPS SN and AIPS CL tables. Task RLDly can generate an AIPS SN table with cross–hand phase and delay differences from a polarized calibrator for either linear or circular feed basis data

With the wide fractional bandwidth of MeerKAT, Faraday rotation is both important and can be measured with sufficient frequency resolution in the imaging. Wideband imager MFImage images in coarse frequency bins whose fractional bandwidth is controlled by parameter maxFBW provides this frequency resolution. Imaging should be done with sufficiently small maxFBW that the needed range of rotation measure (RM) can be determined.

VI. Polarization Calibration

There are two options for polarization calibration of data resulting from the calibration pipeline described in Section IV. These are using a standard calibration or determining the calibration from the dataset in question. Which is preferred depends on the dataset in question and if it contains adequate calibration of a sufficiently polarized calibrator. At present (Jan. 2020) these include 3C286, 3C138, J1130-1449 and J2329-4730. If the dataset contains one of these calibrators, it is better to use the calibration derived from that dataset. If the data does not contain one of these calibrators, the standard calibration is the only option. Supporting scripts and calibration data are available in ftp://ftp.cv.nrao.edu/NRAO-staff/bcotton/MKPoln.

A. Standard Calibration

The standard polarization calibration consist of two tables, an AIPS PD and AIPS BP table containing a suitable set of calibration parameters. These are distributed as fits files in ftp://ftp.cv.nrao.edu/NRAO-staff/bcotton/MKPoln and need to be copied to the visibility dataset in question. Currently, these are MedAvg59.PolCalTab.uvtab.gz (reference antenna 59=m058) and MedAvg61.PolCalTab.uvtab.gz (reference antenna 61=m060). MedAvg61.PolCalTab.uvtab.gz is usable for data prior to Nov. 2019 after which the receiver was replaced.

Data should be calibrated using the calibration pipeline described in Section IV with command line options "–polcal –flags –parms=parmfile" and a file named "parmfile" containing:

```
parms['refAnt'] = 61 # or 59
```

After the calibration is completed, use task TabCopy the copy the tables (PD 2 and BP 1) to the visibility datasets as PD and BP sequence number 1.

B. Calibration using observed calibrators

Determining polarization calibration requires a strong polarized and, preferably, a strong unpolarized source. The parallel hand data should be calibrated using the calibration pipeline described in Section IV with command line options "–polcal –flags". The script may be allowed to pick a reference antenna or force one as described in the previous Section.

Script ftp://ftp.cv.nrao.edu/NRAO-staff/bcotton/MKPoln/MKPolCal.py can be used to calibrate instrumental polarization of the data. Given a uv data file and a list of calibrators, this script will optionally clip the calibrator data, optionally apply a point source phase self calibration, perform instrumental polarization calibration and optionally correct for the apparent EVPA offset. This will leave PD and BP tables on the data suitable for applying in MFImage. This script has a list of known polarized calibrator names and uses these values in the calibration. See the online documentation for details.

The technique described in Section III should give better results but the implementation needs further development.

VII. Imaging

Obit task MFImage can apply the polarization calibration and image in Stokes I,Q,U and V using parameters $Stokes = 'IQUV'$, $doPol = True$, $PDVer = 1$, $doBand = 1$, $BPVer = 1$. See the help and explain sections of the online documention for details about tuning the details of the CLEANing of the polarized emission. The spectral resolution of the output is controlled by parameter $maxFBW$ (maximum fractional bandwidth) whose default value of 5% gives 14 channels across the MeerKAT L band. This allows recovery of rotation measures (RM) up to $\approx \pm 200$ rad/m^2. To cover a wider range of RM decrease $maxFBW$. A value of 2% gives 34 channels in the output.

VIII. Polarization stability

The stability of the MeerKAT polarization after calibration using the noise diodes and the same parallel hand reference antenna(m058) was determined from the analysis of 11 datasets taken over several months. A median average value of each parameter for each antenna was determined by dropping the 25% of the most extreme values and averaging the remainder. The average RMS residual of all measurements of each parameter type over all antennas was determined. The RMS X-Y residual difference was 1.8° , the RMS elipticity residual was 0.00093°, and the RMS orientation residual was 0.028°.

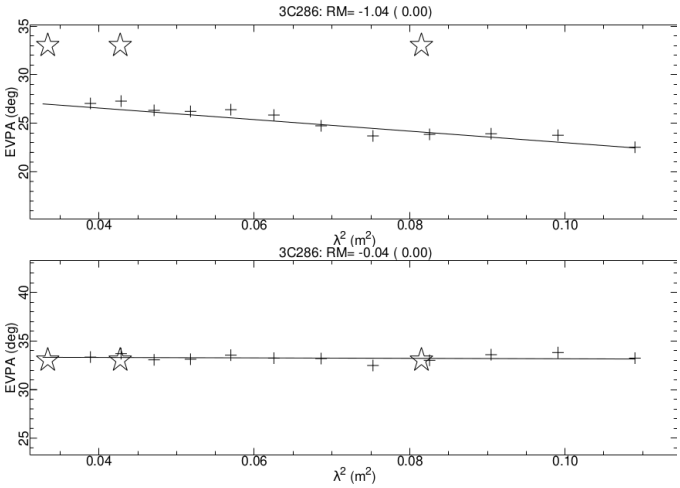

Fig. 1. 3C286 EVPA verses λ^2 from observations taken on 1 Jul 2019. The upper panel has no correction for EVPA applied and the lower has a correction of 7.7° and an RM correction of 1 rad m^{-2}. The '*+ symbols show the MeerKAT measurements, the line is a fitted rotation measure and the stars are the VLA calibration data from [4].

IX. EVPA offset

For reasons that are not completely understood, calibration and imaging of sources with known polarization systematically show an offset of about 8° in the polarization Electric Vector Position Angle (EVPA) with some variation in frequency, see Figure 1, upper panel. A rotation of the orientation of the antenna feeds from the assumed horizontal and vertical would cause a similar EVPA offset but there is little evidence for such a physical rotation seen in the beam holography measurements (M. de Villieurs, private communication). Whatever the cause, corrections can be applied by a frequency dependent rotation of the feed orientations in the calibration AIPS PD table. When an orientation correction is applied corresponding to an EVPA correction of 7.7° with an RM correction of 1 rad m^{-2}, the lower panel in Figure 1 is obtained.

X. Examples

A. Standard calibration of calibrator observation

In order to test the long term polarization stability, a standard set of polarization calibrations derived from 1 Jul 2019 data was applied to data from 27 Nov. 2018 with noise diode and parallel hand calibration done with the script described in Section IV and then imaged in Stokes I, Q, U and V. The results are summarized in Table I with selected RM plots in Figures 2 – 5. Figure 3 shows that the long term stability of the EVPA calibration is quite good, compare with Figure 1. However, the comparison with the VLA calibration values of [4] for 3C138 in Figure 2 shows an EVPA discrepancy of about 4°. J1130-1449 (Fig. 4) and J2329-4730 (Fig. 5) generally exhibit the expected λ^2 dependence of EVPA but with a phase offset at the shorter wavelengths. The Stokes V images generally consist of positive and negative responses more-or-less symmetrically places about the peak Stokes I and are likely artifacts.

TABLE I
STANDARD CALIBRATION OF CALIBRATORS

Source	I	rms	Q	rms	U	rms	frac V	rms	f_L	P	RM
	Jy/bm	mJy/bm	mJy/bm	mJy/bm	mJy/bm	mJy/bm	%	mJy/bm	%,°	mJy/bm	rad m^{-2}
3C48	17.031	0.001	71.6	0.48	-14.0	0.48	+0.09,-0.12	0.51	0.4% @ -6	111	2
3C138	8.763	0.029	584.0	0.15	-17.6	0.012	+0.08,-0.15	0.12	6.6% @ -1	590	-2
J0252-7104	6.092	0.28	-2.59	0.05	-0.35	0.05	+0.01,-0.02	0.05	<0.04%		
J0318+1628	7.774	0.43	15.54	0.13	-3.30	0.15	+0.10,-0.11	0.13	0.2% @ -6	18.1	3
0408-65	15.739	0.38	-0.36	0.11	-3.42	0.12	+0.01,-0.03	0.12	<0.02%		
J0538-4405	3.075	0.51	4.96	0.06	-5.13	0.05	+0.04,-0.01	0.04	0.2% @ -23	17.4	70
J0825-5010	5.629	0.049	5.38	0.07	-6.81	0.09	+0.02,-0.12	0.06	0.2% @ -26	11.2	-2
J0906-6829	1.852	0.26	16.60	0.05	-12.28	0.04	+0.02,-0.07	0.03	1.1% @ +18	45.2	-51
J1008+0740	6.753	1.37	-10.06	1.19	9.65	1.67	+0.07,-0.11	1.22	0.2% @ +68	16.7	2
J1130-1449	4.940	1.07	-136.7	1.26	58.43	1.16	+0.36,-0.16	0.90	3.0% @ +78	243	33
J1619-8418	1.63	0.23	-3.63	0.04	-0.10	0.05	+0.03,-0.05	0.03	<0.2%	6.8	-3
1934-638	14.641	0.75	23.7	0.15	-17.80	0.12	+0.05,-0.04	0.40	0.2% @ -18	49.5	0
J2329-4730	2.898	0.84	64.17	0.10	-12.84	0.06	+0.49,-0.10	0.07	2.2% @ -6	105.67	14

Notes: Stokes I, Q, and U at the position of the calibrator are given with the RMS values for the wideband average.
"frac V" gives the maximum and minimum fractional Stokes V,
"f_L" is the fractional linear polarization and average EVPA, if detected.
"P" and "RM" are the polarized intensity and rotation measure from a rotation measure analysis.

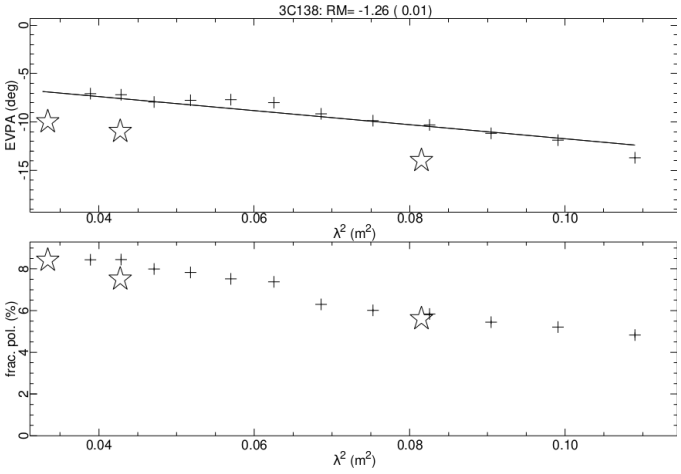

Fig. 2. 3C138 EVPA and fractional linear polarization verses λ^2 from observations taken on 27 Nov. 2018 and polarization calibrated using data taken on 1 Jul 2019. The upper plot is the EVPA v. λ^2 and the '*' symbols show the MeerKAT measurements , the line is a fitted rotation measure and the stars are the VLA calibration data from [4]. The lower plot shows the fractional polarization.

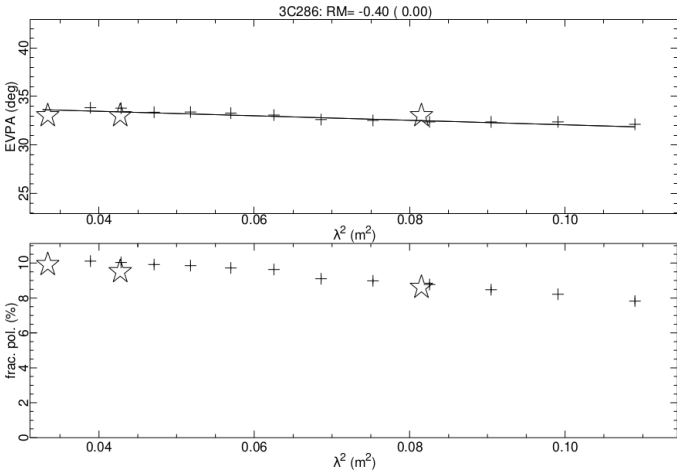

Fig. 3. Like Figure 2 but for 3C286 observed on 24 December 2019, compare with Figure 1.

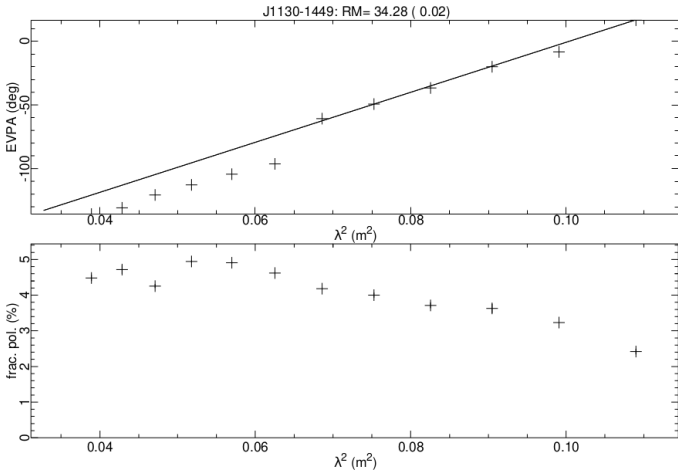

Fig. 4. Like Figure 3 but for J1130-1449.

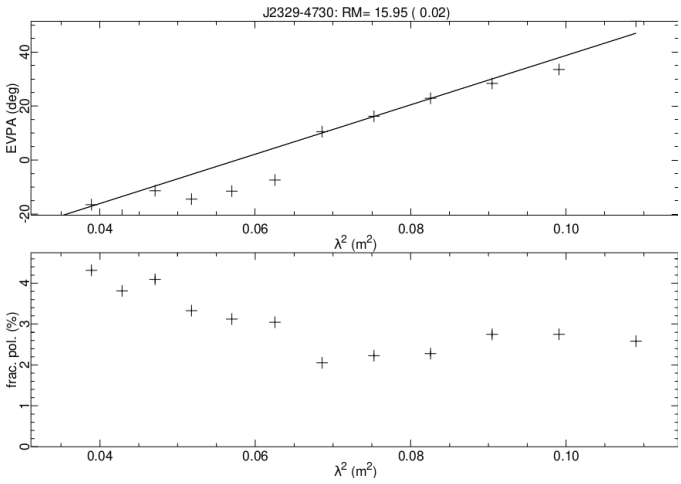

Fig. 5. Like Figure 2 but for J2329-4730.

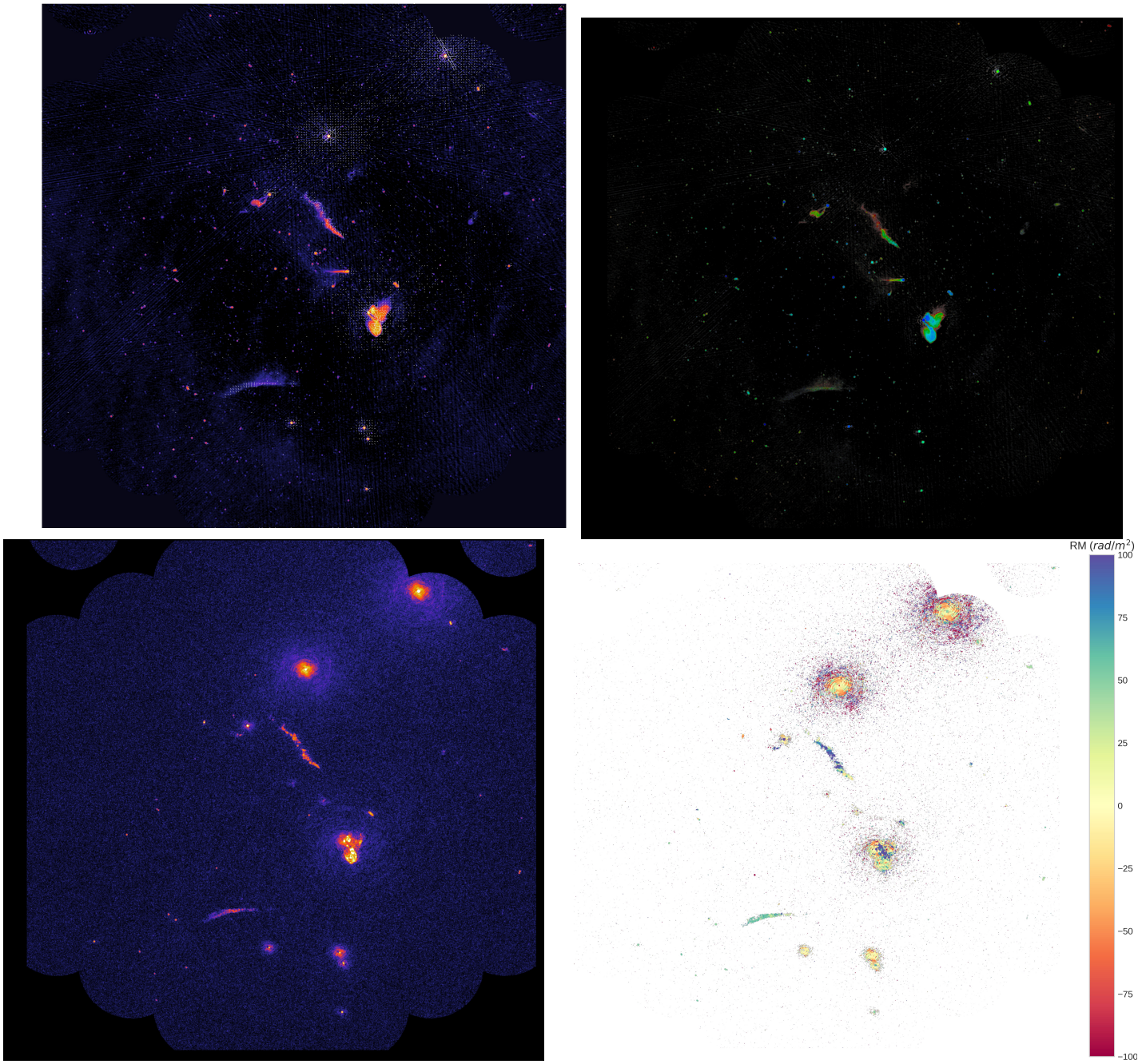

Fig. 6. Galaxy cluster J0431.4-6126. **Upper left:** Total intensity in color with EVPA orientation vectors. **Upper right:** Spectral index as color and total intensity as brightness; red is steeper, blue is flatter. **Lower left:** Polarized intensity as color. **Lower right:** Faraday rotation as color.

B. Galaxy Cluster J0431.4-6126

Deep images of the science verification observation of the region near the galaxy cluster J0431.4-6126 is shown in Figure 6. These images were parallel hand calibrated based on data from that session (3 March 2019) but the polarization calibration was obtained on 1 July 2019.

C. SNR W44

Images of the science verification observation of the region near the super nova remnant W44 is shown in Figure 7. These images were calibrated based on data in the same observing session. This source has a large and rich structure in foreground Faraday rotation.

D. SNR G304.6+0.1

Images of the science verification observation of the region near the super nova remnant G304.6+0.1 is shown in Figure 8. These images were calibrated based on data in the same observing session.

E. Galactic Faraday Screen

Figure 9 gives images of a region several degrees above the Galactic plane showing Galactic Faraday structure in front of

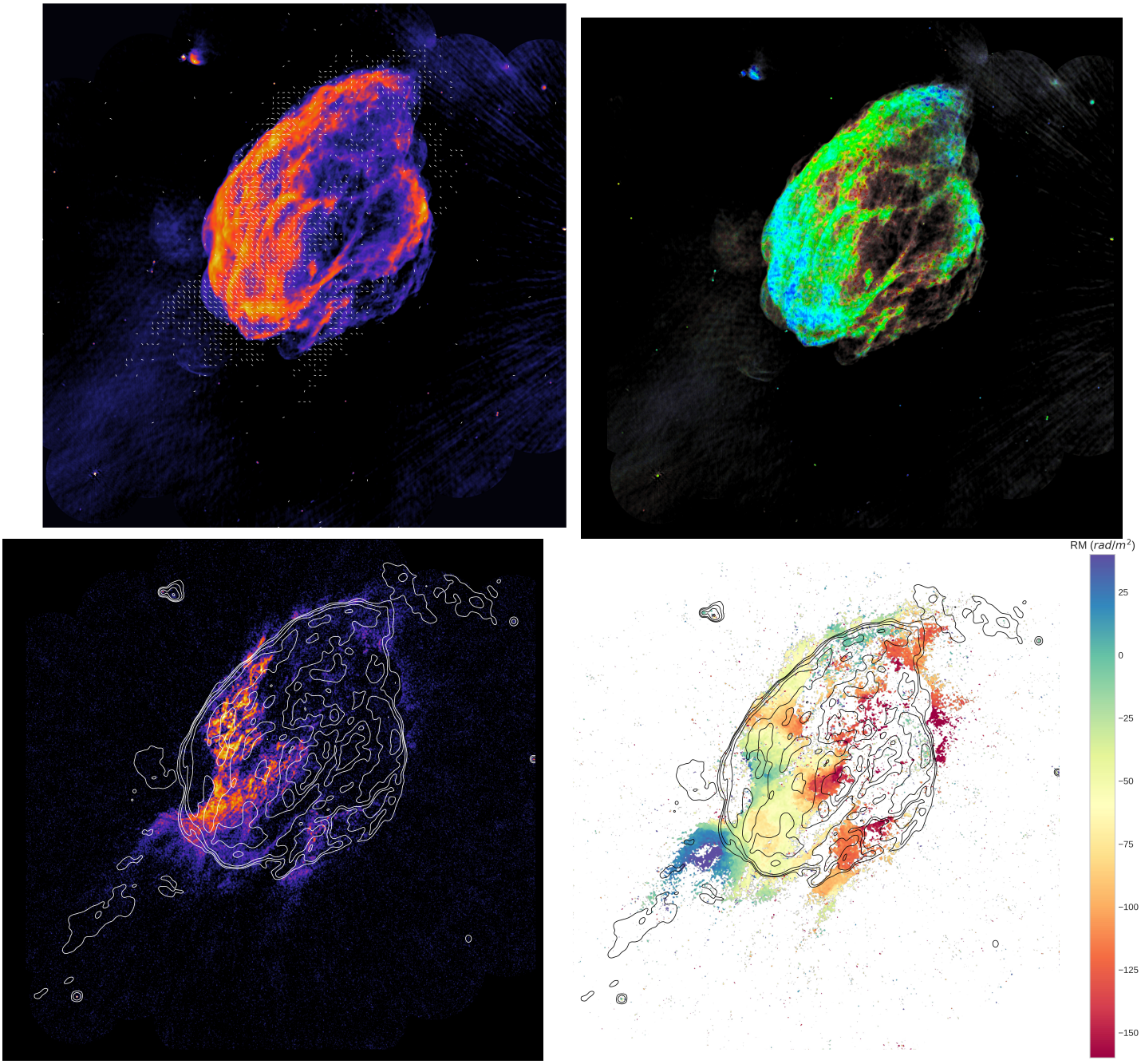

Fig. 7. Super nova remnant W44. **Upper left:** Total intensity in color with EVPA orientation vectors. **Upper right:** Spectral index as color and total intensity as brightness; red is steeper, blue is flatter. **Lower left:** Total intensity as contours and polarized intensity as color. **Lower right:** Total intensity as contours and Faraday rotation as color.

the disk emission which is totally resolved in Stokes I. The finer scale structures in Q and U allow the imaging in polarized light.

XI. Discussion

The polarization properties of MeerKAT, after calibration using the noise diodes at the beginning of each session appear to be stable over many months and calibration of linear polarization is possible even without a polarized calibrator in each dataset. However, each receiver has its own calibration, especially the residual X-Y phase after noise diode calibration. The parallel hand calibration results in the calibration for the reference antenna to be that of the whole dataset. Thus, for data to use a calibration from another dataset, the reference antennas used should be the same. Averaged datasets from multiple observations are available for a select number of reference antennas (Section VI-A).

Errors in the X-Y phase calibratioon will rotate linear into circular polarization. Experiments measuring weak circular polarization in linearly polarized sources need particularly careful calibration of the X-Y phase difference.

Galactic disk Stokes I emission is smooth on scales sampled

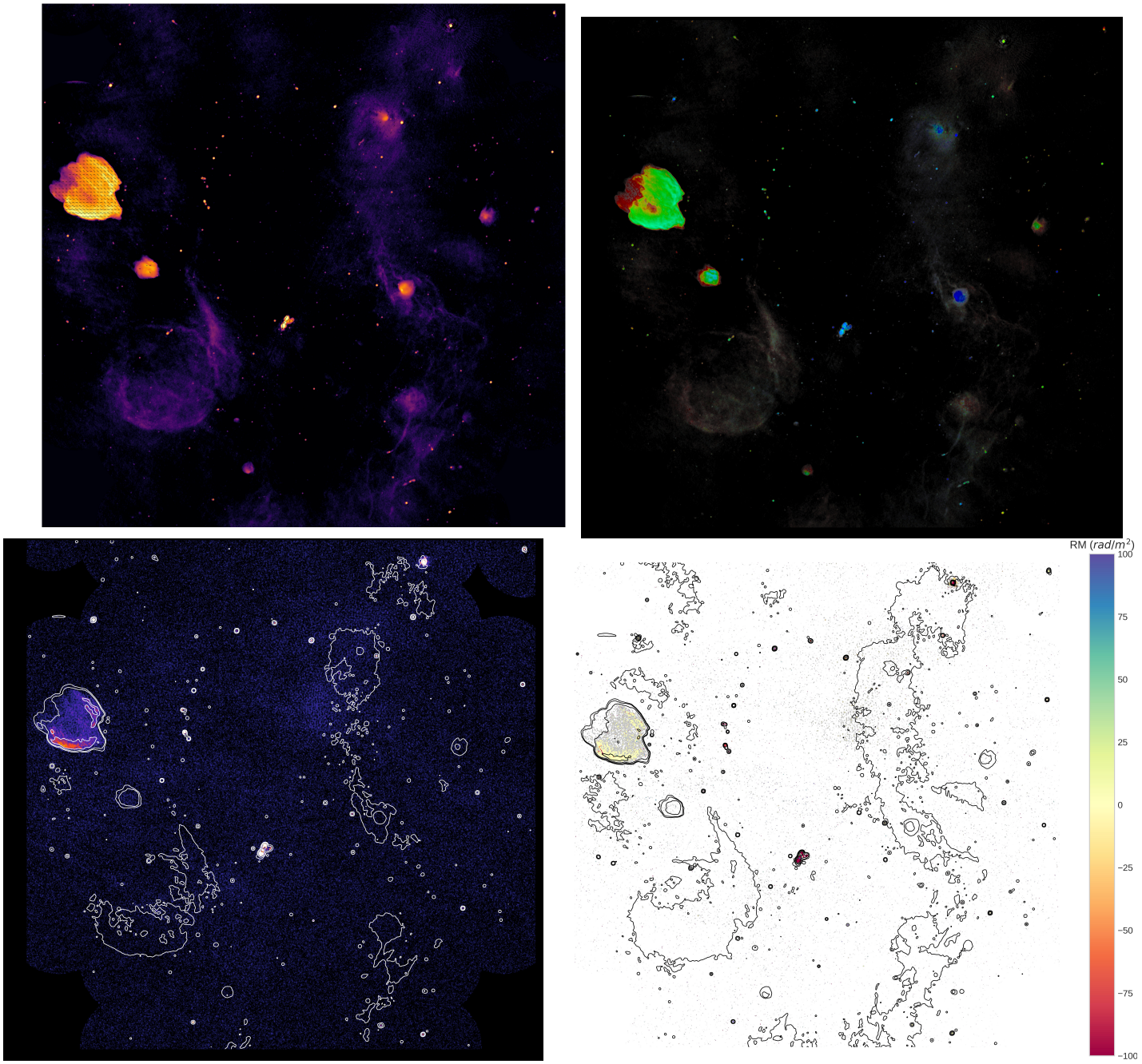

Fig. 8. Super nova remnant G304.6+0.1. **Upper left:** Total intensity in color with EVPA orientation vectors. **Upper right:** Spectral index as color and total intensity as brightness; red is steeper, blue is flatter. **Lower left:** Total intensity as contours and polarized intensity as color. **Lower right:** Total intensity as contours and Faraday rotation as color.

by MeerKAT so completely resolved. However, there are Faraday rotating structures in the ISM on much finer scales and these structures are revealed in the Q and U images. This will complicate using polarized emission to distinguish the emission type of Galactic structures.

ACKNOWLEDGMENT

We would like to thank Mattieu de Villiers for his thoughts on the antenna responses.

REFERENCES

[1] W. D. Cotton, "Obit: A Development Environment for Astronomical Algorithms," *PASP*, vol. 120, pp. 439–448, 2008.

[2] A. R. Thompson, J. M. Moran, and G. W. Swenson, Jr., *Interferometry and Synthesis in Radio Astronomy, 2nd Edition*, Thompson, A. R., Moran, J. M., & Swenson, G. W., Jr., Ed. Wiley-Interscience, 2001.

[3] W. D. Cotton, "On–axis Instrumental Polarization Calibration for Linear Feeds," *Obit Development Memo Series*, vol. 32, p. 11, 2015. [Online]. Available: ftp://ftp.cv.nrao.edu/NRAO-staff/bcotton/Obit/PCalXY.pdf

[4] R. A. Perley and B. J. Butler, "Integrated Polarization Properties of 3C48, 3C138, 3C147 and 3C286," *ApJS*, vol. 206, p. 16, 2013.

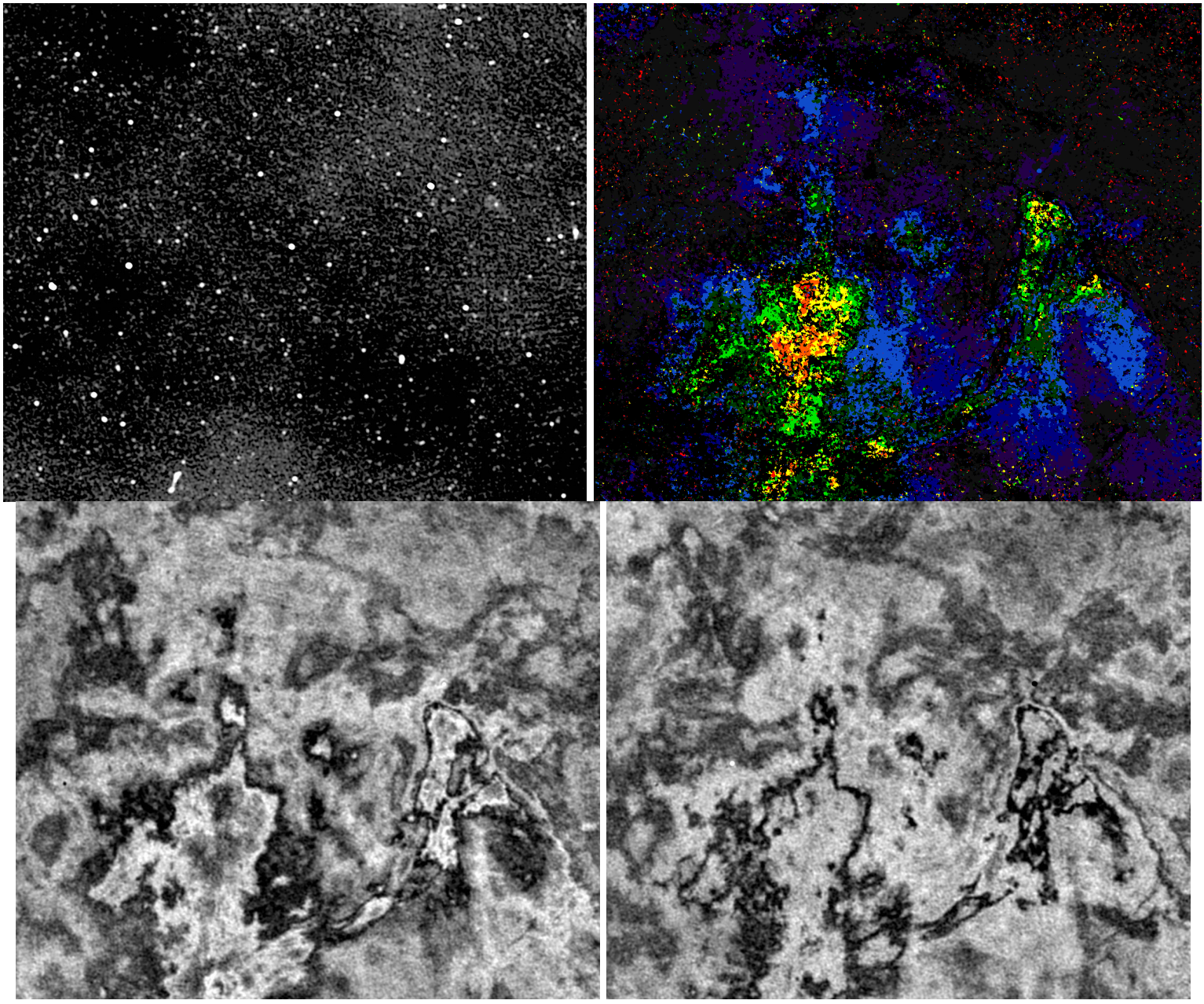

Fig. 9. Segment of the Galactic Faraday screen, shows $0.5^\circ \times 0.4^\circ$ **Upper left:** Total intensity -30 to 200 μJy/bm **Upper right:** Rotation measure in color, range $\pm$80 rad/m^2. **Lower left:** Stokes Q $\pm$80 μJy/bm. **Lower right:** Stokes U $\pm$80 μJy/bm.